LNAPL Infiltration in the Vadose Zone: Comparisons of Physical and Numerical Simulations

MARINA PANTAZIDOU
Department of Civil and Environmental Engineering, Carnegie Mellon University

ABSTRACT

The numerical model T2VOC was used to reproduce light, nonaqueous phase liquid (LNAPL) infiltration scenarios in the vadose zone. The numerical modeling results were compared to results from laboratory experiments simulating LNAPL spills in the vadose zone. Laboratory measurements included results from one-dimensional column and two-dimensional tank experiments using uniform sands of varying average grain sizes. The constitutive relationships for the sands were obtained from the one-dimensional experiments. The two-dimensional experiments simulated leakage of kerosene under constant head. The sensitivity of the numerical results to the constitutive relationships used and the specified boundary conditions was examined. For this purpose two different capillary pressure-saturation relationships were used for the same sand and both constant head and constant flux conditions were simulated. The constant head boundary conditions resulted in significantly greater contaminant front speeds than those observed experimentally. Within the contaminated area, different LNAPL saturations were obtained for the two capillary pressure curves used. The constant flux boundary conditions produced a much better prediction. At the initial stages of infiltration the results for both capillary pressure curves were similar and in good agreement with the experimental results. However, as the LNAPL front approaches the capillary fringe the choice of the capillary pressure curve was found to influence the results.

INTRODUCTION

Numerical models are indispensable in the study of immiscible fluid transport because the equations that describe multiphase fluid flow are strongly coupled and highly non-linear, and thus do not admit analytical solutions, except for specific problems in which simplifying assumptions are possible [e.g., one-dimensional displacement of oil by water (Buckley and Leverett, 1942)]. Modeling efforts include solutions for two-phase flow, i.e., water and NAPL (Hochmuth and Sunada, 1985; Osborne and Sykes, 1986; Kueper and Frind, 1991a,b) and for three-phase flow systems, i.e., water, NAPL, and air (Faust, 1985; Abriola and Pinder, 1985a,b; Kaluarachchi and Parker, 1989; Falta et al., 1992a). Validation of these codes, by comparison to field or laboratory data, has been very limited mainly due to the scarcity of such data (Lenhard et al., 1988; Faust et al., 1989; Falta et al., 1992b). In the absence of laboratory or field data, and given our present limited understanding of the migration potential of NAPLs, we can only hypothesize on the dimensional and time scales associated with NAPL transport processes. Examples of the questions we need to answer include: how long it will take an LNAPL to reach the water table? how far horizontally will the LNAPL spread? This paper investigates the effect of two factors, namely the boundary conditions specified and the constitutive relationships selected, on the answers that a numerical model might give to the aforementioned questions. The numerical code used, T2VOC (Falta et al., 1994), is an adaptation of the STMVOC simulator developed at Lawrence Berkeley Laboratory by R. Falta and K. Pruess (Falta and Pruess, 1991). The following sections describe briefly the experiments that are used for comparison and the results of the numerical simulations.

EXPERIMENTAL SIMULATIONS

One-dimensional drainage experiments were conducted in order to determine the constitutive relationships, which are required for numerical modeling of NAPL migration, using a procedure developed by Pantazidou (1991). Capillary pressure and relative permeability curves were determined for a fine and a coarse sand. The relative permeability curves obtained for the two sands were almost identical, confirming Wyckoff and Botset's (1936) early observation that relative permeability curves for sands are not affected by permeability magnitude. These relative permeability curves were also in good

agreement with Wyllie's (1962) formula, which expresses the relative permeability as a function of the third power of the scaled saturation (Pantazidou and Sitar, 1993). The capillary pressure curves were different for the two sands, as expected, since these curves reflect variations in particle or, equivalently, pore size distribution. Guided by these observations, the sensitivity of the numerical results to the input capillary pressure curves was examined in this study.

The two-dimensional experiments simulated LNAPL spills in unsaturated, two-dimensional domain above the water table. The procedure for the two-dimensional tests consisted of releasing red-dyed kerosene in the unsaturated zone, after a water table had been established within the sand sample. The dimensions of the sand sample were 61 cm by 61 cm by 5 cm. The evolution of the front was observed through the transparent side of the tank containing the sample and the contaminant front was traced at appropriate intervals. Visual observations were supplemented by pressure measurements of water and kerosene and by water saturation measurements. A total of fifteen tests was conducted to investigate the effects on NAPL transport of soil grain size, heterogeneities, and water table fluctuations. Detailed description of the materials used, the test procedures and the results is presented elsewhere (Pantazidou and Sitar, 1993). In this paper, one experiment on a uniform, fine sand sample was selected for comparison with the numerical results. The capillary pressure curve for this fine sand (measured points on Figure 1) was found to be approximated well by a van Genuchten type curve with α=3.157 and n=8.09 (curve C on Figure 1). Figure 2 shows contaminant front profiles at different times for this experiment. A total of 350 cm^3 of kerosene was allowed to infiltrate in the sand sample under a constant head of 4 cm of kerosene. Under this constant head, kerosene infiltration lasted for about 3 hours, corresponding to an average flux of 2.4 cm^3/min.

NUMERICAL SIMULATIONS

Four numerical simulations are selected for discussion in this paper reproducing constant head and constant flux boundary conditions for two different capillary pressure curves. The constant LNAPL head was specified to be the same as the constant kerosene head that was maintained in the physical simulations, i.e., 4 cm of kerosene. The constant LNAPL flux was calculated as an average of the actual flux that was observed in the experiments during kerosene infiltration under the 4-cm constant head, i.e., 2.4 cm^3 of kerosene per minute. The choice of the capillary pressure-saturation curve determines the volume of water retained in the pore space above the water table and is therefore expected to affect the LNAPL transport patterns in the unsaturated domain. Simulations using the best-fit van Genuchten capillary pressure curve ran into convergence problems associated with the steep rise in capillary pressure for saturations close to 100 percent (see curve C on Figure 1). Ongoing work is addressing these issues. In the meantime, simulations were performed with two alternative curves, A and B (see Figure 1). Curve A was selected because it produces an average water saturation (or water volume) above the water table that is comparable to the measured distribution (i.e., curve C on Figure 1). Curve B has been suggested in the literature (ES&T, Inc., 1990) for sands, and results in a very low water volume above the water table.

The constant head simulations, although better representing the experimental boundary conditions, resulted in very high contaminant front speeds. Figures 3a and 3b show LNAPL saturation profiles at 15 minutes after the beginning of infiltration; the experimentally observed contaminant front is also highlighted for comparison. It is interesting to note that the use of capillary curve B (lower water saturation above the water table) results in a deeper contaminated area (Figure 3b) and also in significantly higher LNAPL saturations within the contaminated area. Whereas the difference in saturation cannot be discerned from the black-and-white plots, inspection of the saturation output values shows a maximum LNAPL saturation beyond the leaking source of approximately 85 percent for the low water content case (curve B) compared to a maximum saturation of only 55 percent for the high water content case (curve A). As a result, the total volume of LNAPL in the sample is significantly larger for initial conditions of low water content, the difference increasing with time.

The constant flux simulations produced a much better agreement with the experimental results. Figures 4a and 4b show contaminant profiles after 30 minutes of kerosene infiltration. These figures show that the results for curves A and B do not differ significantly and are in good agreement with the observed contaminant fronts also shown on these figures. Output saturation values indicate that during the initial stages of infiltration, kerosene is mainly displacing air and, as a result, is not significantly affected by the contrast between the water saturation for the two cases. Upon careful inspection, a trend for lateral spreading can be discerned from the results obtained using curve A (higher water saturation above the water table).

The difference between the results obtained using the two curves increases at later stages of infiltration, as can be seen from Figures 5a and 5b, which present experimental and numerical results after 120 minutes of kerosene infiltration. The numerical simulations failed to accurately capture the horizontal spreading of the contaminant, the difference being more pronounced for the low initial water saturation case (Figure 5b). The dramatic contrast observed between calculated LNAPL saturations within the contaminated area for the curves A and B in the constant head simulations was not reproduced for the constant flux boundary conditions. However, the saturation distribution within the contaminated area exhibited different trends for the two cases. For the high water content initial conditions, the maximum saturations occupied a small portion of the contaminated area, close to the leaking source, whereas for the low water content condition, a significant portion of the affected area was contaminated at saturations close to the maximum value calculated. It is also interesting to note that the total contaminated area for the high initial water content was 20 percent larger compared to the low water content case. The predicted difference is in agreement with experimental results showing that during infiltration in the unsaturated zone, high initial water content conditions result in a larger contaminated area at lower LNAPL saturations compared to low initial water content conditions, for the same volume of contaminant release (Pantazidou and Sitar, 1993).

SUMMARY

These initial results indicate that the choice of boundary conditions can have a dramatic impact on the predicted mobility of NAPLs. In this study the constant head conditions failed to reproduce a realistic contaminant flux. Furthermore, the distribution of water in the unsaturated zone, as determined by the capillary pressure-saturation relationships, can affect significantly the results and therefore necessitates determination of the capillary pressure curve that corresponds to the soil type of interest. Perhaps the most important conclusion is that in the absence of experimental results, we may obtain several sets of numerical results that will look reasonable without having any way of telling which ones are realistic.

Acknowledgments. The unfailing assistance of Stefan Finsterle and Karsten Pruess of Lawrence Berkeley Laboratory and Jason Buesing of Carnegie Mellon University is greatly appreciated.

REFERENCES

Abriola, M., and G.F. Pinder, 1985a, A Multiphase Approach to the Modeling of Porous Media Contamination by Organic Compounds, 1, Equation Development, Water Resour. Res., 21:1:11-18.

Abriola, L.M., and G.F. Pinder, 1985b, A Multiphase Approach to the Modeling of Porous Media Contamination by Organic Compounds, 2, Numerical Simulation, Water Resour. Res., 21:1:19-26.

Buckley, S.E., and M.C. Leverett, 1942, Mechanism of Fluid Displacement in Sands, Trans. AIME, 146:107-116.

Environmental Systems & Technologies, Inc. (ES&T, Inc.), 1990, MOFAT: A Two Dimensional Finite Element Program for Multiphase Flow and Multicomponent Transport, Program Documentation - Version 2.0, Blacksburg, Virginia.

Falta, R.W., and K. Pruess, 1991, STMVOC User's Guide, Lawrence Berkeley Laboratory Report LBL-30758, Berkeley, CA.

Falta, R.W., K. Pruess, I. Javandel, and P.A. Witherspoon, 1992a, Numerical Modeling of Steam Injection for the Removal of Nonaqueous Phase Liquids From the Subsurface: 1. Numerical Formulation, Water Resour. Res. 28:2:433-449.

Falta, R.W., K. Pruess, I. Javandel, and P.A. Witherspoon, 1992b, Numerical Modeling of Steam Injection for the Removal of Nonaqueous Phase Liquids From the Subsurface: 2. Code Validation and Application, Water Resour. Res. 28:2:451-465.

Falta, R.W., K. Pruess, S. Finsterle, and A. Batistelli, T2VOC User's Guide, draft report, October 1994.

Faust, C.R., 1985, Transport of Immiscible Fluids Within and Below the Unsaturated Zone: A Numerical Model, Water Resour. Res., 21:4:587-596.

Faust, C.R., J.H. Guswa, and J.W. Mercer, 1989, Simulation of Three-phase Flow of Immiscible Fluids Within and Below the Unsaturated Zone, Water Resour. Res., 25:12:2449-2464.

Hochmuth, D.P., and D.K. Sunada, 1985, Ground-water Model of Two-phase Immiscible Flow in Coarse Material, Ground Water, 23:5:617-626.

Kaluarachchi, J.J., and J.C. Parker, 1989, An Efficient Finite Element Method for Modeling Multiphase Flow, Water Resour. Res., 25:1:43-54.

Kueper, B.H., and E.O. Frind, 1991a, Two-phase Flow in Heterogeneous Porous Media, 1, Model Development, Water Resour. Res., 27:6:1049-1057.

Kueper, B.H., and E.O. Frind, 1991b, Two-phase Flow in Heterogeneous Porous Media, 2, Model Application, Water Resour. Res., 27:6:1059-1070.

Lenhard, R.J., J.H. Dane, J.C. Parker, and J.J. Kaluarachchi, 1988, Measurement and Simulation of One-dimensional Transient Three-phase Flow for Monotonic Liquid Drainage, Water Resour. Res., 24:6:853-863.

Osborne, M., and J. Sykes, 1986, Numerical Modeling of Immiscible Organic Transport at the Hyde Park Landfill, Water Resour. Res., 22:1:25-33.

Pantazidou, M., 1991, Migration of Nonaqueous Liquids in Partly Saturated Granular Media, PhD Thesis, University of California, Berkeley.

Pantazidou, M., and N. Sitar, 1993, Emplacement of Nonaqueous Liquids in the Vadose Zone, Water Resour. Res., 29:3:705-722.

Wyckoff, R.D., and H.G. Botset, 1936, The Flow of Gas-Liquid Mixtures through Unconsolidated Sands, Physics, (J. Appl. Phys.), 7:9:325-345.

Wyllie, M.R.J., 1962, Relative Permeability, Chapter 25 of Vol.2 in: Petroleum Handbook, Frick, T.C. Ed., SPE of AIME, Dallas, Texas.

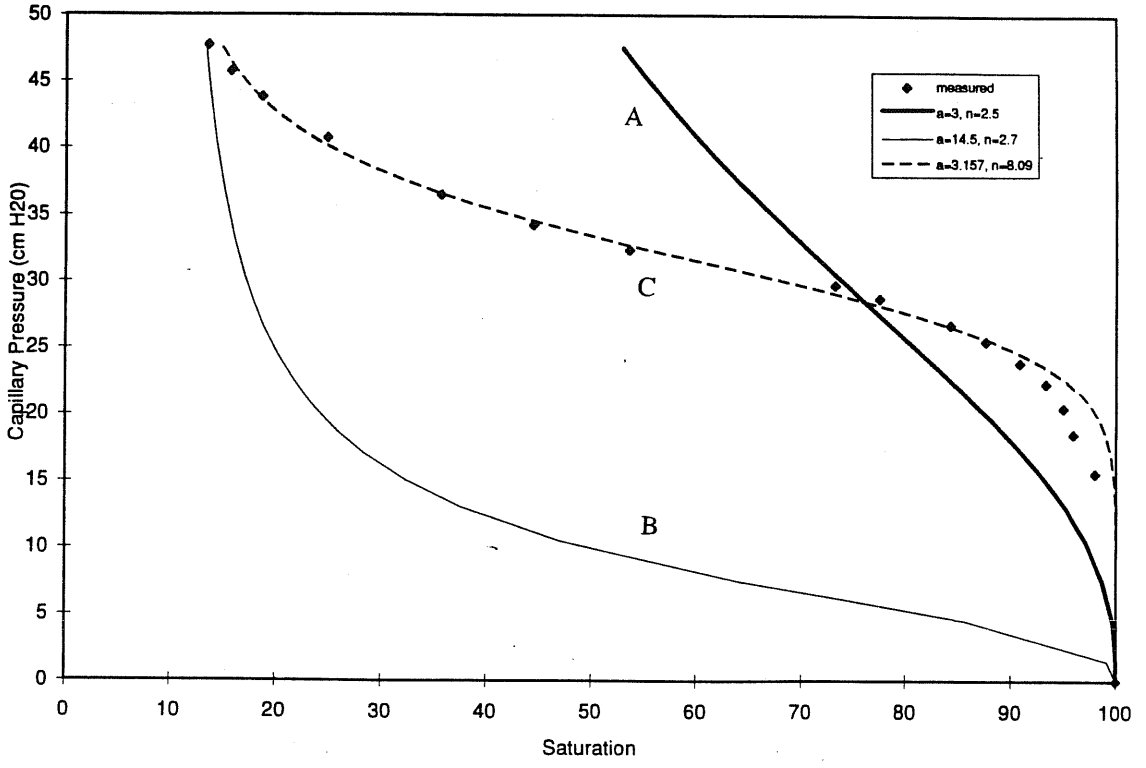

Fig. 1. Capillary pressure-saturation curves for different a and n parameters and measured values for fine sand.

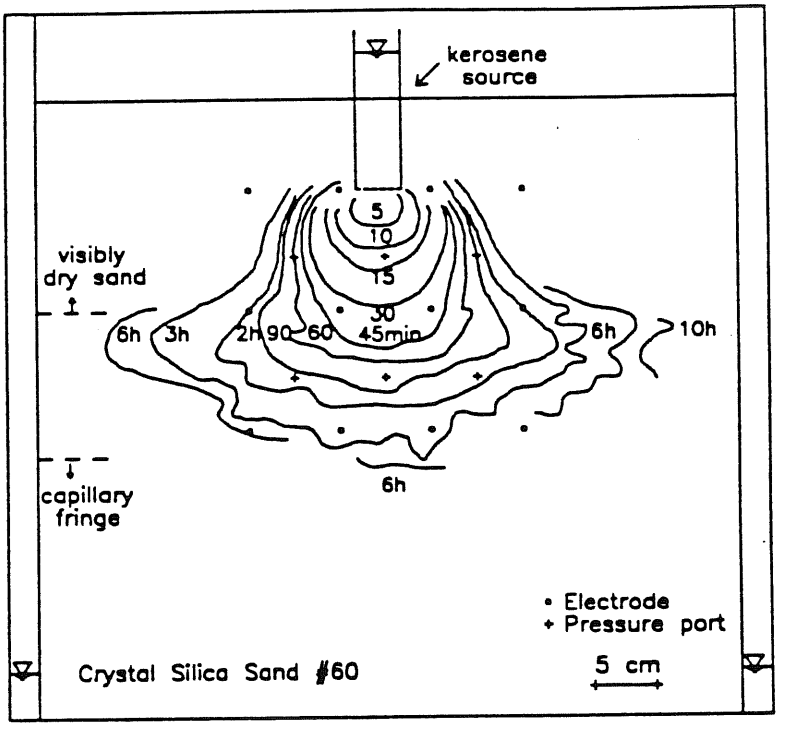

Fig. 2 . Observed kerosene front propagation for fine sand.

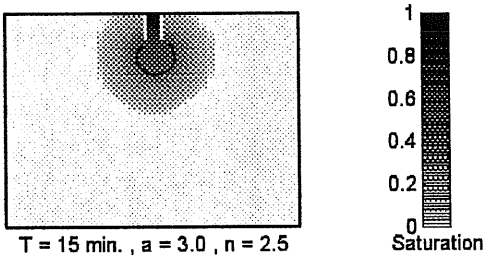

Figure 3a: Simulated kerosene front at 15 minutes using capillary pressure curve A and constant head.

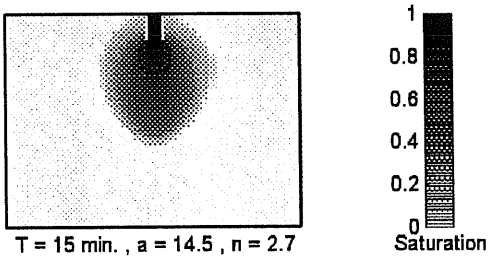

Figure 3b: Simulated kerosene front at 15 minutes using capillary pressure curve B and constant head.

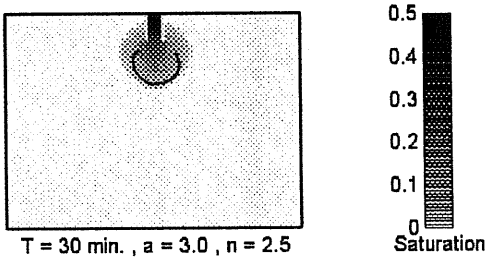

Figure 4a: Simulated kerosene front at 30 minutes using capillary pressure curve A and constant flux.

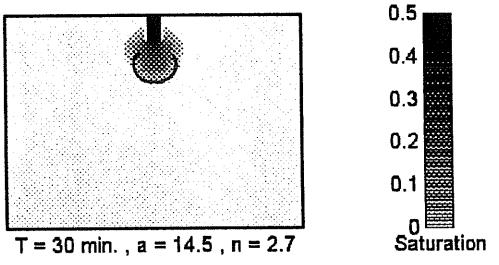

Figure 4b: Simulated kerosene front at 30 minutes using capillary pressure curve B and constant flux.

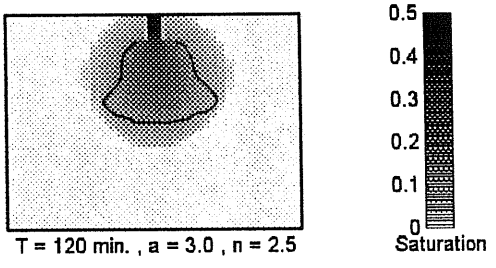

Figure 5a: Simulated kerosene front at 120 minutes using capillary pressure curve A and constant flux.

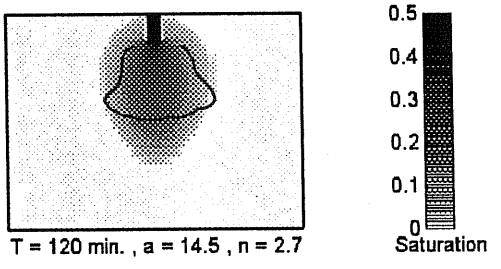

Figure 5b: Simulated kerosene front at 120 minutes using capillary pressure curve B and constant flux.